Resisting Dune Erosion with Bio-cementation

Brina M. Montoya[1], T. Matthew Evans[2], Meagan E. Wengrove[3], Hailey Bond[4], Pegah Ghasemi[5], Ehsan Yazdani[6], Ali Dadashiserej[7], Qianwen Liu[8]

[1]Department of Civil, Construction, and Environmental Engineering, North Carolina State University, Raleigh, NC 27695, USA; e-mail: bmmorten@ncsu.edu Corresponding author.
[2]School of Civil and Construction Engineering, Oregon State University, Corvallis, OR 97331, USA; e-mail: matt.evans@oregonstate.edu
[3]School of Civil and Construction Engineering, Oregon State University, Corvallis, OR 97331, USA; e-mail: meagan.wengrove@oregonstate.edu
[4]School of Civil and Construction Engineering, Oregon State University, Corvallis, OR 97331, USA; e-mail: bondh@oregonstate.edu
[5]Department of Civil, Construction, and Environmental Engineering, North Carolina State University, Raleigh, NC 27695, USA; e-mail: pghasem@ncsu.edu
[6]School of Civil and Construction Engineering, Oregon State University, Corvallis, OR 97331, USA; e-mail: ehsan.yazdani@oregonstate.edu
[7]School of Civil and Construction Engineering, Oregon State University, Corvallis, OR 97331, USA; e-mail: dadashia@oregonstate.edu
[8]Department of Civil, Construction, and Environmental Engineering, North Carolina State University, Raleigh, NC 27695, USA; e-mail: qliu19@ncsu.edu

ABSTRACT

Coastal dunes often present the first line of defense for the built environment during extreme wave surge and storm events. In order to protect inland infrastructure, dunes must resist erosion in the face of these incidents. Microbial induced carbonate precipitation (MICP), or more commonly bio-cementation, can be used to increase the critical shear strength of sand and mitigate erosion. To evaluate the performance of bio-cemented dunes, prototypical dunes consisting of clean poorly graded sand collected from the Oregon coast were constructed within the Large Wave Flume at the O.H. Hinsdale Wave Research Laboratory at Oregon State University. The bio-cementation treatment was sprayed onto the surface of the unsaturated dune. The level of cementation was monitored using shear wave velocity measurements throughout the duration of the treatments. The treated and control dunes were subjected to 19 trials of approximately 300 waves each, with each trial increasing in water depth, wave height, and wave period. The performance of the dune was evaluated using lidar scans between each wave trial. The results indicate that the surface spraying treatment technique produced consistent levels of bio-cementation throughout the treated length of the dune and demonstrated significant resistance to erosion from the wave trails.

INTRODUCTION

Coastal dunes are often the first line of defense for the built environment during extreme wave surge and storm events; as such, dunes must resist erosion in the face of these incidents. The resiliency of coastal dunes corresponds to the ability of a community to rebound after an extreme event. As seen on the Outer Banks of North Carolina, Highway 12 needs to be repaired or rebuilt after nearly every hurricane or nor'easter that reaches its shores (Carr 2016). This in turn cuts communities off until the highway is repaired. If coastal dunes are reinforced, more infrastructure may remain operational during an extreme event and the loss to communities due to the downtime to recover and rebuild is reduced.

Microbial induced carbonate precipitation (MICP), or more commonly bio-cementation, can be used to reinforce unsaturated coastal sand dunes and improve their resistance to erosion. Natural soil bacteria are used to induce calcium carbonate to precipitate, bonding sand grains together and increasing the shear strength and resistance (DeJong et al. 2010). Bio-cementation has successfully been implemented in unsaturated sand environments (Cheng 2013), and has demonstrated resistance to erosion from surface flow and wave action (Do et al. 2019, Shanahan and Montoya 2016). Collectively, these experimental results indicate that bio-cementation is an effective method to reduce material loss from erosion, and generally a threshold level of mineral precipitation is needed for effective mitigation. However, the research assessing the erodibility of bio-cementation to date has focused on element- and model-scale experiments. The work presented herein evaluates the effectiveness of bio-cementation within prototypical dunes consisting of clean poorly graded sand collected from the Oregon coast, constructed within the Large Wave Flume (LWF) at the O.H. Hinsdale Wave Research Laboratory (HWRL) at Oregon State University. Bio-cementation was implemented through a surface spraying system that had previously been implemented in field conditions (Ghasemi and Montoya 2020). The bio-cemented dune was subjected to 19 trials of approximately 300 waves each representing wave conditions throughout the peak of a hurricane. The performance of the dune was evaluated using lidar scans between each wave trial. The resulting bio-cemented material and its resistance to erosion from wave loading in the LWF are discussed.

MATERIALS AND METHODS

Dune Sand. Fifty-six dump trucks (~1,000 m^3) of sand were sourced from the Oregon coast and delivered to the O.H. Hinsdale Wave Research Laboratory at Oregon State University. The sand has a specific gravity of 2.67, D_{50} = 0.18 mm, and minimum and maximum void ratios of 0.57 and 0.78, respectively. The sand was placed in lifts and compacted in the LWF using vibratory plate compactors to achieve a density similar to dunes along the Oregon Coast, as assessed by dynamic cone penetrometers (DCP). DCP was used in accordance to ASTM D6951-09 (2015) to provide an empirical indication of shear strength. DCP consists of an 8-kg sliding hammer that

falls on a 111-cm shaft, driving the cone connected to it into the ground. Penetration depth is recorded after each drop and penetration index (PI) is expressed in terms of cm/blow.

Bio-cementation Treatment Process. *Sporosarcina pasteurii* (ATCC 11859), a common soil bacterium, was used to catalyze bio-cementation reactions. The bacteria were cultured in an aerobic environment at 30 degrees Celsius in filter-sterilized ammonium-yeast media (ATCC medium 1376) until the optical density (OD_{600}) was between 0.8-1.0. Once the bacteria reached the target optical density, 40 L of suspended bacteria were then mixed with 450 L of 300 mM urea to inoculate the dune sand as described below.

The MICP treatment was applied to the dune through a series of sprayers that evenly distribute the media to the surface of the dune (Figure 1). This system consisted of two sets of 24 nozzles with a 32 and 58 cm spacing from the walls and each other, respectively, in the width direction of flume, and 30 cm between two nozzles along the length of the flume. The spray nozzles were fed by a main hose connected to a transfer pump that pulled from a 1041 L (275 gallon) tank used to prepare and store the solution. The solution in the tank was pumped through the main hose from the bottom to the top of the slope and recirculated back to the tank. Each nozzle had a working pressure of 69-138 kPa and a maximum discharge rate of 32.55 l/hr at an inlet pressure of 138 kPa. A valve at the end of the recirculation line was used to adjust the fluid pressure throughout the system to provide 138 kPa pressure and, therefore, a consistent distribution of solution throughout the surface. The bio-cementation surface spraying method was delivered to one-third of the width of the dune within the LWF, as shown in Figure 1. A mass stabilization method to implement bio-cementation was used in another third of the dune, with a buffer untreated zone in the middle third of the dune. Measurements from the mass stabilized portion of the dune are not discussed in the current work.

Figure 1. Surface spraying treatment setup.

A two-phase treatment method with chemical recipes shown in Table 1 was used to treat the dune. Bacteria were inoculated to the soil with biological solution and after a retention time of at least 3 hours the cementation solution was percolated into the soil. The biological solution only contained urea to avoid immediate precipitation of the calcium carbonate. The cementation solution was prepared with 3:1 ratio of urea to calcium chloride based on previous studies to optimize the recipe (Ghasemi et al. 2019). Each treatment consisted of 450 L of either biological or cementation solution; treatments were delivered as shown in Table 2. In this table B_i and C_i denote biological and cementation solutions respectively.

Table 1. Chemical recipe for biological and cementation solution.

Constituents	Biological solution	Cementation solution
Urea	300 mM	300 mM
$CaCl_2$	---	100 mM

Table 2. Bio-cementation treatment schedule.

Day	Treatments	Treatment Duration (min)
1	B_1, C_1	30, each
2	C_2, C_3, C_4, B_2	30, each
3	C_5, C_6, C_7, C_8	30, each
4	B_3, C_9, C_{10}	30-45, each
5	C_{11}, C_{12}, B_4	30-45, each
6	C_{13}, C_{14}, C_{15}	30-45, each
7	C_{16}, C_{17}, B_5	30-45, each
8	C_{18}, C_{19}, C_{20}	30-45, each
9	C_{21}, B_6, C_{22}	30-45, each
10	C_{23}, C_{24}	30-45, each
	Washed with water	

The bio-cementation process was monitored using shear wave velocity measures via bender element sensors. Piezoelectric bender elements (Piezo Systems, MA) were embedded in the sand approximately 10 cm below the final surface of the dune. A bender element pair was framed by a fiber paper to maintain the tip-to-tip distance of the sensors as 15 cm during testing without providing a mechanism for wave propagation at speeds faster than the embedment medium. A 10-V sinusoidal wave with a frequency sweep of 1–20 kHz was supplied by a function generator (Agilent 33522A) and received by a digital oscilloscope (Agilent MSO6014A). The tip-to-tip distance was divided by the time associated with the first arrival of the received signal to calculate the shear wave velocity. The shear wave velocity was measured immediately before each treatment and at the conclusion of the treatment schedule.

Wave Conditions. The treated and control dunes were subjected to irregular waves simulating the storm surge and increase in wave height and period throughout the peak of a hurricane. Wave conditions were determined by scaling data and model results from conditions during Hurricane Sandy and discretizing them into 19 trials of approximately 300 waves each. The irregular waves were generated using a TMA spectrum.

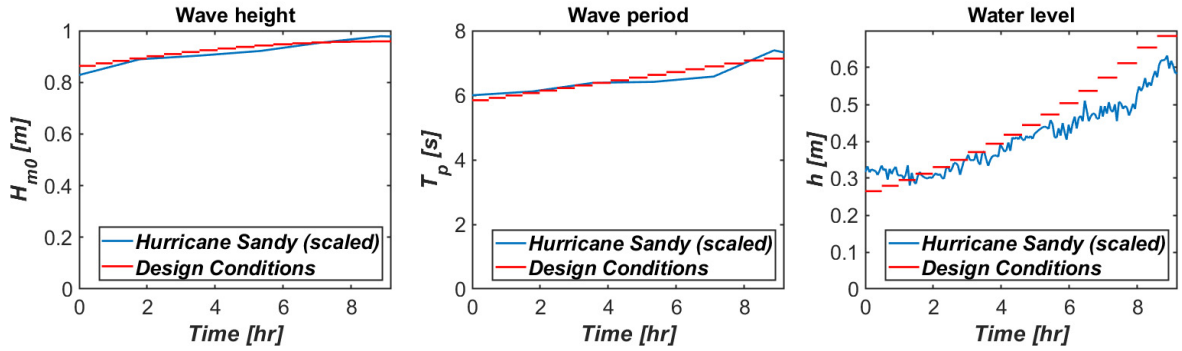

Figure 2. Wave Characteristics.

Erodibility Assessment. A submerged impinging jet was used to evaluate the erodibility of the cemented soil surface following Khanal et al. (2016) and ASTM (2017).

The applied shear stress, τ_i, is calculated following Al-Madhhachi et al. (2013):

$$\tau_{\mathrm{i}} = C_{\mathrm{f}}\rho_{\mathrm{w}}U^2\left(\frac{C_{\mathrm{d}}d_0}{J_{\mathrm{i}}+s}\right)^2 \quad (1)$$

where, C_f is the coefficient of friction (0.00416, Hanson and Cook 2004), ρ_w is the fluid density (tap water, 1000 kg/m^3), U is shear velocity at the nozzle as a function of head differential (h), C_d is the diffusion constant (6.3, Hanson and Cook 2004), d_0 is nozzle diameter, J_i is the initial distance between the nozzle and original soil surface, and s is the scour depth due to the impinging jet. The pressure head (i.e., h) was increased until scour was initiated, and the induced scour and corresponding time were recorded. When no more erosion is induced, the applied shear stress is taken as the critical shear stress (τ_c). The scour depth and time were used to calculate the erosion rate (e.g., $\varepsilon_{r(i)} = [s_{(i+1)}–s_{(i)}]/[t_{(i+1)}–t_{(i)}]$) and corresponding applied shear stress (e.g., $\tau_{i(i)} = [\tau_{i(i+1)}+\tau_{i(i)}]/2$). Finally, the erodibility coefficient (k_d) and the exponent (α) were determined from the relationship between $\varepsilon_{r(i)}$, $\tau_{i(i)}$ and τ_c given in Eq. (2) using the least square curve fitting approach.

$$\varepsilon_{\mathrm{r}} = k_{\mathrm{d}}(\tau_{\mathrm{i}} - \tau_{\mathrm{c}})^{\alpha} \quad (2)$$

Performance of Dune: Lidar scans were used to assess the performance of the dunes under wave action. Lidar is a remote assessment technology that uses a laser beam to measure variable distances to an object. The laser scanner provides a non-contact measurement system that assesses the travel time of an emitted continuous light or pulse from the transmitter to an object and back. The distance traveled between the scanner and the object is computed using travel time and the

speed of light. The output of the scans is a point cloud consisting of a dataset of points in space with known x, y and z coordinates which are the captured geometry and texture features of the scanned region. The lidar scanners used in this erosion monitoring study were a Leica scan station P40 and a BLK360.

The dune was scanned before the wave inundation and the acquired point cloud was used as a reference. The point dataset collected after each wave action was compared with the reference point cloud. CloudCompare software (Girardeau-Montaut, D. 2016).]was used to process the 3D point clouds and generate a triangular mesh for rendering images. In order to detect the changes in 3D geometric data, a triangular mesh was generated from the reference point cloud (i.e., prior to waves) and compared with the point clouds acquired after wave trial scanning. Mesh to cloud distance measurements allow for the quantification of the amount of eroded material.

Calcium Carbonate Content Measurement. After finishing the treatment process, samples were taken from locations where the jet test was performed to facilitate measurement of cementation level of the soil. Samples were oven dried and then soaked in a 1-M HCl solution. The solution was then extracted carefully with syringe and this process was repeated until no bubbles were detected. Then the samples were oven dried again and the mass difference was recorded. The mass of calcium carbonate was calculated as the percentage of the dissolved calcium carbonate over the mass of oven dried soil.

RESULTS

Bio-cementation Treatment. The surface spraying method resulted in a consistent bio-cemented crust along the entire length of the treated dune, as seen in Figure 3. The average shear wave velocity of the bio-cemented sand was 1100 m/s, with the minimum and maximum shear wave velocity of 1040 m/s and 1290 m/s, respectively. This is in contrast to the average shear wave velocity of the untreated sand of 100 m/s. The average mass of carbonate measurements for the bio-cemented crust was approximately 1.2% ± 0.8%. The thickness of the bio-cemented crust ranged from at least 15 to 43 cm. The PI values from the DCP within the bio-cemented crust were 2.12 ± 2 cm/blow, while the untreated sand PI values were 7.0 ± 4.4 cm/blow.

Erodibility Parameters. The submerged impinging jet results indicate the erodibility of the bio-cemented sand increases as a function of the mass of carbonate. The critical shear stress for the untreated sand ranged from 0.11 to 0.25 Pa while the bio-cemented sand exhibited a critical shear stress in the range of 60 to 128.97 Pa (Figure 4a). The associated Shields parameter for the untreated sand is between 0.04 to 0.08 and between 20 and 50 for bio-cemented sand (Figure 4b). The erodibility coefficient (k_d) decreases as mass of carbonate increases; untreated sand was on the order of $10^5\ mm/(hr \cdot Pa)$ and decreases to the order of $10\ mm/(hr \cdot Pa)$ (Figure 4c). The α exponent ranges from 0.5 to 1.5 for the specimens tested without a clear trend with regards to

the mass of carbonate (Figure 4d). Collectively, the erodibility parameters assessed indicate that the bio-cemented sand is much more resistant to erosion compared to the untreated sand.

The applied shear stress and erosion rate for each specimen was plotted on the proposed erodibility chart by Briaud (2013). The initial applied shear stress after the occurrence of scour and the corresponding initial erosion rate are presented in Figure 5. The untreated specimens demonstrate "very high erodibility" or an erodibility level equivalent to that of sand, while the bio-cemented sand specimens demonstrate "medium erodibility" or an erodibility level equivalent to that of high plastic silts and lean clay. This evolution of erodibility resistance with bio-cementation proved to be sufficient to resist significant wave loading in the LWF.

Figure 3. Bio-cemented dune during testing (right) adjacent to the untreated buffer zone (left).

Dune Performance under Wave Loading. Lidar scan data is another measure of the efficacy of the surface treatment during wave action. Lidar data rendering of the dune surface has been presented in Figure 6. By comparing the eroded region of the untreated buffer zone with the treated slope, the resistance of the surface treated zone in the face of the wave surges is clearly evident.

In Figure 6, blue represents the eroded region whereas red indicates sand accumulation. Figure 6(a) and (b) depict the actual and scan data of the dune after Trial 6. Moderate erosion and slight sand accumulation occurred in the untreated buffer zone at the toe and middle of the slope, respectively. Maximum erosion occurred at the toe of the dune where the surface treated zone ends

due to the wave collision with the cemented crust, while in the untreated buffer zone, the waves have a longer travel distance due to the lack of energy dissipation at the toe and greater infiltration, resulting in more uniform erosion that travels much further upslope. Figure 6(c) and (d) indicate the dune condition during and after 15 trials. The eroded region in the untreated buffer zone reached the middle of the dune with more than 0.25 m of erosion. Figure 6(e) and (f) shows the treated slope remained largely intact after 22 trials and indicates significant resistance to erosion, while the buffer untreated zone exhibits an escarpment line of approximately 0.65 m in depth with significant erosion throughout the length of the untreated buffer zone. By considering Figure 6, the progressive geomorphologic deterioration in the untreated buffer zone is obvious as the wave trials progressed while the surficial crust created by the surface spraying treatment technique decreased the vulnerability of the dune and enhanced the erosion mitigation.

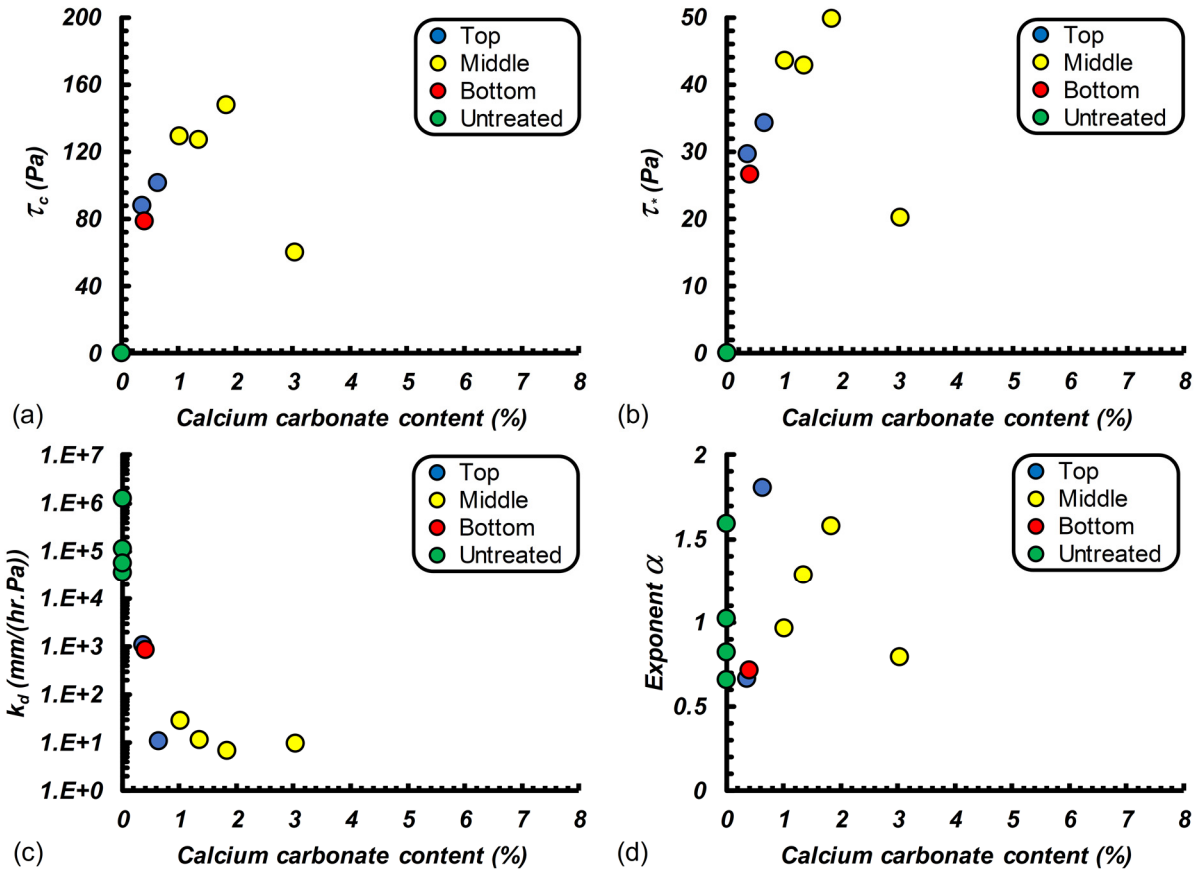

Figure 4. Erodibility parameters results: a) critical shear strength, b) shields parameter, c) k_d, d) α (i.e., exponent in Equation 2).

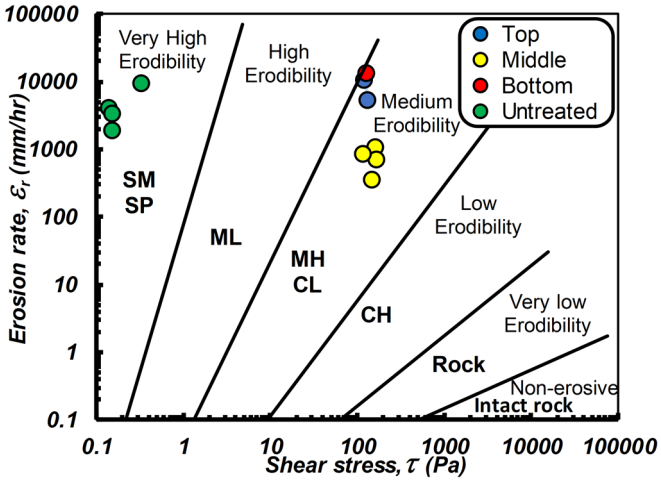

Figure 5. Erosion rate-initial shear stress relationship with erodibility chart proposed by Briaud (2013).

CONCLUSION

Bio-cementation was successfully implemented with a prototypical unsaturated dune within the LWF. The bio-cementation was implemented using a surface spraying approach that resulted in a stiff cemented crust ranging approximately 15 to 43 cm in thickness across the treated area. The level of cementation was assessed via shear wave velocity and mass of carbonate measurements. The measured shear wave velocities were relatively uniform across the length of the treated area with the average value assessed to be 1100 m/s. The corresponding mass of carbonate measurements were approximately 1.2% ± 0.8%. The consistency of the bio-cemented dune was also assessed using dynamic cone penetrometer (DCP) penetration indices (PI), which showed PI values of 2.12 ± 2 cm/blow within the cemented zones; this is in contrast to the baseline untreated zone that had PI values of 7.0 ± 4.4 cm/blow. The erodibility parameters of the bio-cemented sand are influenced by the level of cementation; generally, the critical shear stress increases and the erodibility coefficient decreases as the mass of carbonate increases. In particular, the critical shear stress increased from values less than 1 kPa to around 100 kPa for the bio-cementation level implemented in the dune. The lidar data indicates that the surface treatment increased the erosion resistance in face of wave loading compared with the untreated zone that experienced 0.65 m of erosion at the end of the trial 22. These results indicate that bio-cementation may be a viable option to mitigate dune erosion.

ACKNOWLEDGEMENTS

This material is based upon work supported by the National Science Foundation under Grant Numbers CMMI-1519679, 1933350, and 1933355. Any opinions, findings, and conclusions or recommendations expressed are those of the authors and do not necessarily reflect the views of the

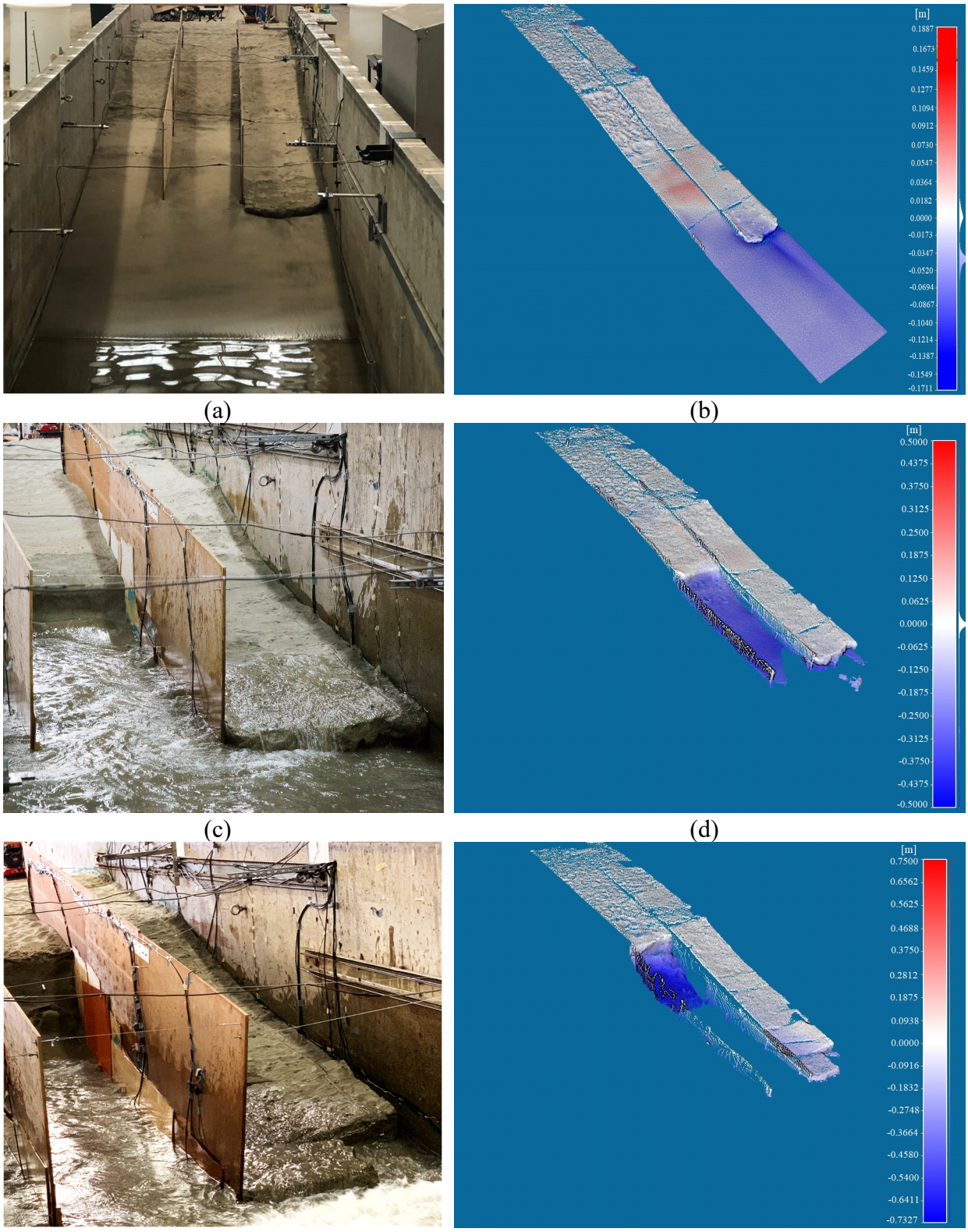

Figure 6. (a) Dune surface after trial #6, (b) Scanned surface after trial #6 (c) Dune surface during trial #15, (d) Scanned surface after trial #15, (e) Dune surface during trial #22, and (f) Scanned surface after trial #22

National Science Foundation. The physical modeling described herein was performed in the Large Wave Flume at the O.H. Hinsdale Wave Research Laboratory at Oregon State University and would not have been possible without the significant support, assistance, and expertise of the HWRL staff.

REFERENCES

Al-Madhhachi, A.-S. T., Hanson, G. J., Fox, G. A., Tyagi, A. K., and Bulut, R. (2013). "Measuring Soil Erodibility Using a Laboratory 'Mini' JET." *Transactions of the ASABE*, American Society of Agricultural and Biological Engineers, 56(3), 901–910.

ASTM. (2015). "D6951-09 Standard Test Method For Use Of The Dynamic Cone Penetrometer In Shallow Pavement Applications." ASTM International, West Conshohocken, PA.

ASTM. (2017). "D5882 Standard Test Method for Erodibility Determination of Soil in the Field or in the Laboratory by the Jet Index Method." ASTM International, West Conshohocken.

Briaud, J. L. (2013). *Geotechnical engineering: unsaturated and saturated soils*. John Wiley & Sons.

Carr, D. (2016). NC 12: Gateway to the Outer Banks. University of North Carolina Press, Chapel Hill, NC.

Cheng, L., Cord-Ruwisch, R., Shahin, M.A. (2013). "Cementation of sand soil by microbially induced calcite precipitation at various degrees of saturation." *Canadian Geotechnical Journal*, 50, 81-90.

DeJong, J.T., Mortensen, B. M., Martinez, B. C., and Nelson, D. C. (2010). "Bio-mediated soil improvement." *Ecological Engineering*, 36(2), 197–210.

Do, J., Montoya, B.M., Gabr, M.A. (2019). "Debonding of MICP-Stabilized Sand by Shearing and Erosion." *Geomechanics and Engineering*, 17(5).

Ghasemi, P., Montoya, B.M. (2020). "Field Application of the Microbially Induced Calcium Carbonate Precipitation on a Coastal Sandy Slope." *Proceedings from ASCE Geo-Congress 2020*, Minneapolis, MN, ASCE Geotechnical Special Publication.

Girardeau-Montaut, D. (2016). "CloudCompare".

Hanson, G. J., and Cook, K. R. (2004). "Apparatus, test procedures, and analytical methods to measure soil erodibility in situ." *Applied Engineering in Agriculture*, 20(4), 455–462.

Khanal, A., Fox, G. A., and Al-Madhhachi, A. T. (2016). "Variability of Erodibility Parameters from Laboratory Mini Jet Erosion Tests." *Journal of Hydrologic Engineering*, 21(10), 04016030.

Shanahan, C., Montoya, B.M. (2016). "Erosion Reduction of Coastal Sands using Microbial Induced Calcite Precipitation." *Proceedings from ASCE Geo-Chicago 2016 Conference*, Chicago, Illinois, ASCE Geotechnical Special Publication 269, 42-51.